

Artificial synaptic behavior of the SBT-memristor

Gang Dou(窦刚), Ming-Long Dou(窦明龙), Ren-Yuan Liu(刘任远), and Mei Guo(郭梅)†

Citation: Chin. Phys. B, 2021, 30 (**7**): 078401. DOI: 10.1088/1674-1056/ac05a3
Journal homepage: http://cpb.iphy.ac.cn; http://iopscience.iop.org/cpb

What follows is a list of articles you may be interested in

SBT-memristor-based crossbar memory circuit

Mei Guo(郭梅), Ren-Yuan Liu(刘任远), Ming-Long Dou(窦明龙), and Gang Dou(窦刚)
Chin. Phys. B, 2021, 30 (**6**): 068402. DOI: 10.1088/1674-1056/abd7dc

Suppression of ferroresonance using passive memristor emulator

S Poornima
Chin. Phys. B, 2021, 30 (**6**): 068401. DOI: 10.1088/1674-1056/abd7e0

Optoelectronic memristor for neuromorphic computing

Wuhong Xue(薛武红), Wenjuan Ci(次文娟), Xiao-Hong Xu(许小红), Gang Liu(刘钢)
Chin. Phys. B, 2020, 29 (**4**): 048401. DOI: 10.1088/1674-1056/ab75da

Switching mechanism for TiO_2 memristor and quantitative analysis of exponential model parameters

Wang Xiao-Ping, Chen Min, Shen Yi
Chin. Phys. B, 2015, 24 (**8**): 088401. DOI: 10.1088/1674-1056/24/8/088401

Toward the complete relational graph of fundamental circuit elements

Shang Da-Shan, Chai Yi-Sheng, Cao Ze-Xian, Lu Jun, Sun Young
Chin. Phys. B, 2015, 24 (**6**): 068402. DOI: 10.1088/1674-1056/24/6/068402

Artificial synaptic behavior of the SBT-memristor*

Gang Dou(窦刚), Ming-Long Dou(窦明龙), Ren-Yuan Liu(刘任远), and Mei Guo(郭梅)†

College of Electrical Engineering and Automation, Shandong University of Science and Technology, Qingdao 266590, China

(Received 31 March 2021; revised manuscript received 29 April 2021; accepted manuscript online 27 May 2021)

The synapse of human brain neurons is not only the transmission channel of information, but also the basic unit of human brain learning and information storing. The artificial synapse is constructed based on the $Sr_{0.97}Ba_{0.03}TiO_{3-x}$ (SBT) memristor, which realizes the short-term and long-term plasticity of the synapse. The experiential learning and non-associative learning behavior in accordance with human cognitive rules are realized by using the SBT-memristor-based synapse. The process of synaptic habituation and sensitization is analyzed. This study provides insightful guidance for realization of artificial synapse and the development of artificial neural network.

Keywords: memristor, artificial synapse, synaptic plasticity, experiential learning, non-associative learning

PACS: 84.32.−y, 07.05.Mh **DOI:** 10.1088/1674-1056/ac05a3

1. Introduction

Researchers have paid considerable attention to the key link of artificial neural network (ANN) to realize human brain bionics, namely, the bionic synapse.[1] For the brain, learning and memory are regarded to be achieved by adjusting the synaptic weights between the two neurons.[2] Synaptic weights can be enhanced or suppressed by external stimulus signals, which is called synaptic plasticity.[3–6] The simulation of synaptic plasticity is considered as the key step of neuromorphic calculations.[7–11]

Memristor known as memory resistor is the fourth passive electronic component after resistors, capacitors and inductors. It is firstly presented by Professor Chua in 1971.[12] However, the physical realization of the memristor has not made a breakthrough due to the limitation of the processing technology. Until 2008, the first memristor is developed by HP labs, which consists of a double-layered TiO_2 film.[13] In recent years, the exploitation of memristive devices as synapses has stimulated a growing interest.[14] The artificial synapses are realized by memristive devices, such as Y_2O_3, TaO_x, HfO_2, WO_x, and MoS_2.[15–21] The advantages of memristors being applied as synapses are due to their fast switching speed, low power consumption, crossbar integration, and analog resistance switching properties,[22–27] which make the memristive synapses as a suitable device for variety applications, including pattern recognition,[28,29] novel storage,[30,31] neuromorphic systems,[32–35] and image processing.[36]

In the paper, the artificial synapse is constructed based on the $Sr_{0.97}Ba_{0.03}TiO_{3-x}$ (SBT) memristor, which realizes the short-term and long-term plasticity of the synapse. Moreover, the experiential learning and non-associative learning behavior in accordance with human cognitive rules are realized by using the SBT-memristor-based synapse. Finally, the process of synaptic habituation and sensitization is analyzed.

2. Construction of a mathematical model for SBT-memristor

The improved SBT memristor is prepared by radio frequency (RF) magnetron sputtering[37]. For electrical measurements, the Agilent B2900 source-measure unit is used to test the current–voltage (i–u) characteristics and the result is shown in Fig. 1.

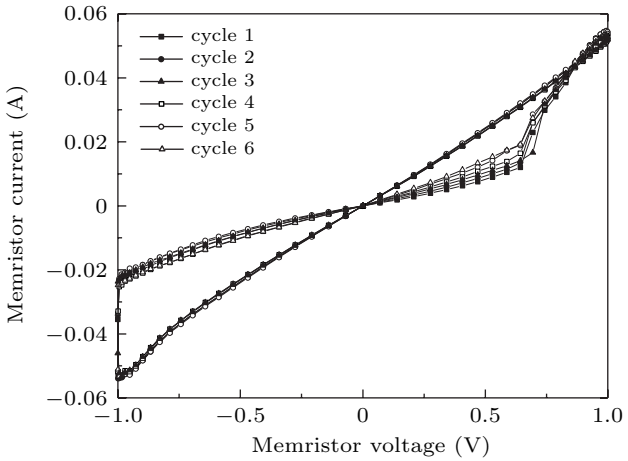


Fig. 1. The measured i–u characteristic curves of SBT-memristor.

When the data of the voltage biases and the corresponding current passing through the SBT-memristor are obtained, they are preprocessed by the subsection-average method. The measured data are divided into several subsections according to their period at first, and then the subsections are further overlaid and averaged. After the preprocessing, the i–u characteristic curves of the SBT-memristor are plotted in Fig. 2.

*Project supported by the National Natural Science Foundation of China (Grant Nos. 61703246 and 61703247), the Qingdao Science and Technology Plan Project (Grant No. 19-6-2-2-cg), and the Elite Project of Shandong University of Science and Technology.

†Corresponding author. E-mail: m.guo@sdust.edu.cn

© 2021 Chinese Physical Society and IOP Publishing Ltd

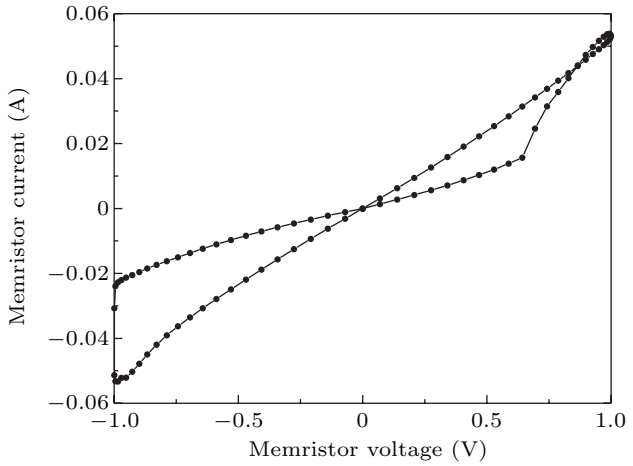


Fig. 2. The *i*–*u* characteristic curve of the SBT-memristor after the preprocessing.

Next, the charge q and the magnetic flux φ across the SBT-memristor could be obtained using the preprocessed voltage and current data in Fig. 2. The results (discrete points) in the first quadrant of q and φ are shown in Fig. 3. Then the φ–q curve (solid line) can be obtained by the curve fitting method of quadratic polynomial according to the discrete data of charge q and magnetic flux φ,[38] as shown in Fig. 3. The φ–q formula of SBT-memristor is as follows:

$$q_1 = 0.0198{\varphi_1}^2 + 0.03308\varphi_1 + 0.003, \tag{1}$$

where

$$u(t) = \frac{\mathrm{d}\varphi(t)}{\mathrm{d}t}, \tag{2}$$

$$i(t) = \frac{\mathrm{d}q(t)}{\mathrm{d}t}, \tag{3}$$

$$w(\varphi) = \frac{i(t)}{u(t)}, \tag{4}$$

and the menductance of SBT-memristor is described as

$$w(\varphi) = 0.03972\varphi_1 + 0.03308. \tag{5}$$

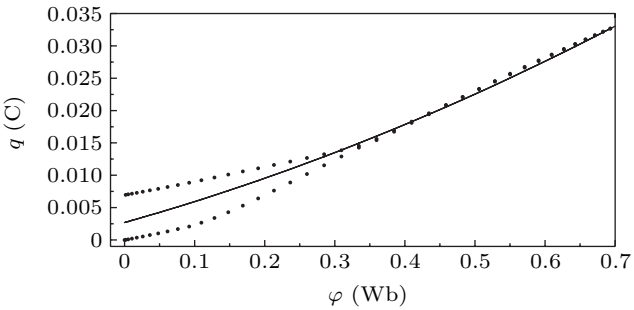


Fig. 3. The data of charge q and magnetic flux φ across the SBT-memristor (discrete points) and the approximated φ–q curve (solid line) in the first quadrant.

The SBT-memristor is a type of metal-semiconductor-metal memristor. The Schottky barrier and the tunnelling current are formed in the metal-semiconductor-metal memristor upon the application of a positive voltage.[39] As Eq. (5) cannot fully characterize the Schottky barrier and tunneling current of SBT-memristors, a new mathematical model in Ref. [39] is introduced. The memristor equations can now be described as

$$i = (1-w)\alpha[1-\exp(-\beta u)] + w\gamma\sinh(\delta u), \tag{6}$$

$$\mathrm{d}w/\mathrm{d}t = \lambda\sinh(\eta u) - \frac{w}{\tau}, \tag{7}$$

where Eq. (6) is the *i*–*u* equation which includes the Schottky term (1st term) and the tunneling term (2nd term).

In Ref. [40], taking into account the change in ion concentration caused by the oxidation-reduction reaction on the surface of electrode, Eq. (7) is improved as

$$\frac{\mathrm{d}w}{\mathrm{d}t} = \lambda\sinh(\eta u) - \frac{w-\mu}{\tau}, \tag{8}$$

where

$$\frac{\mathrm{d}\tau}{\mathrm{d}t} = a\sinh(\eta u), \tag{9}$$

$$\frac{\mathrm{d}\mu}{\mathrm{d}t} = b\sinh(\eta u)f(w), \tag{10}$$

$$f(w) = 0.25\big[(\mathrm{sgn}(u)+1)(\mathrm{sgn}(1-w)+1) + (\mathrm{sgn}(u)+1)(\mathrm{sgn}(w)+1)\big]. \tag{11}$$

Herein, α is prefactor for Schottky barrier, β is exponent for Schottky barrier, γ is prefactor for tunneling, δ is exponent for tunneling. τ and μ are diffusion time constants, u is the applied voltage, w is the menductance value, and i is the current.

The initial values of w, τ, μ are 0.0315, 0.5 and 0.032, respectively. The measured voltage, the measured current, and the menductance value of the SBT-memristor are applied in Eq. (8). The fitting results are $\alpha = -0.0043$, $\beta = 1.4817$, $\gamma = 0.4645$, $\delta = 1.7479$, $\eta = 4$, $\lambda = 0.0021$, $a = 0.001$, and $b = 0.002$.

Under the voltage bias with amplitude 1.0 V, the *i*–*u* characteristic curve (red line) of the SBT-memristor is simulated numerically using the mathematical model (5), (6), (8)–(11), as shown in Fig. 4. The measured *i*–*u* characteristic curves (black line) of the physical SBT-memristor are shown in Fig. 4,

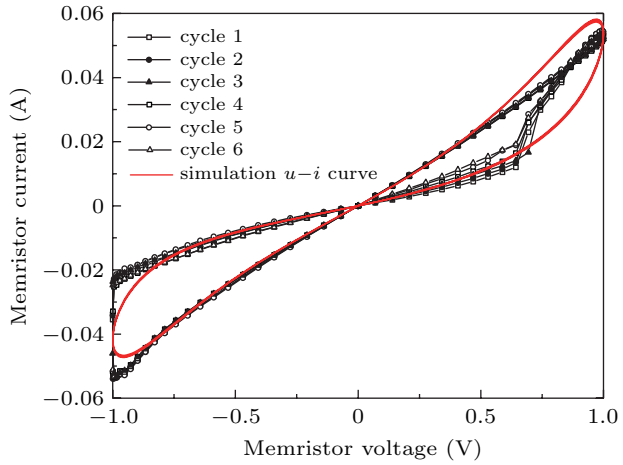


Fig. 4. The comparison of the *i*–*u* characteristic curve simulated from the mathematical model (5), (6), (8)–(11) (red line) and the measured *i*–*u* characteristic curves (black line) of the SBT-memristor.

which indicates that the simulated *i*–*u* characteristic curve is coincident with the measured *i*–*u* characteristic curves of the SBT-memristor well. Thus, the mathematical model (5), (6), (8)–(11) with the definite parameters could be used to characterize the SBT-memristor.

3. Synaptic plasticity

When the memristor is stimulated by the applied voltage, its menductance values change continuously, which is analogous to the synaptic weights in neuromorphic systems.[41–43] When the continuous pulses are applied on synapses, the synaptic weights gradually increase.[44] Consequently, the menductance values of memristor can be taken as the synaptic weight of neuromorphic systems in order to simulate synaptic plasticity.

Here 15 pulses with amplitude of 1.6 V, pulse width of 0.05 s and time interval of 0.05 s are applied to SBT-memristor (see Fig. 5). Under the stimulation of high frequency pulses, the charge carriers in the memristor gradually increase, resulting in the increase of menductance value, which corresponds to the learning process of synapses (blue square). After the pulse is removed, the current values of the memristor decrease. The menductance values go through a process of rapid decline, which is similar to the forgetting process of human brain. This corresponds to the forgetting process of synapses (red circle).

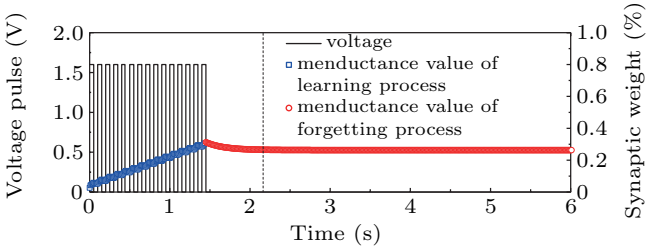


Fig. 5. The simulation of long/short term synaptic plasticity based on SBT-memristor.

The process of synaptic forgetting can be divided into the short-term synaptic plasticity (STP) and the long-term synaptic plasticity (LTP) according to the rate of forgetting. The process of rapid decline for menductance values corresponds to the STP, which is short-term memory. When the amount of charge carriers in the memristor is stable, the current and menductance values are stable, which correspond to the retention of human memory. This process is the LTP, which is long-term memory. Therefore, the attenuation process of menductance value of SBT-memristor is similar with forgetting curve of human brain, and the SBT-memristor can simulate long-term/short-term synaptic plasticity (see Fig. 5).

Then 30 and 40 pulses with amplitude of 1.6 V, pulse width of 0.05 s and time interval of 0.05 s are applied to the memristor, respectively (see Fig. 6). The final menductance values are 0.26, 0.49 and 0.64, respectively, corresponding to 15, 30, and 40 pulses (see Figs. 5 and 6). The synaptic weights increased as more pulses are applied. This demonstrates that short-term memory can be transformed into long-term memory by continuous learning and training.

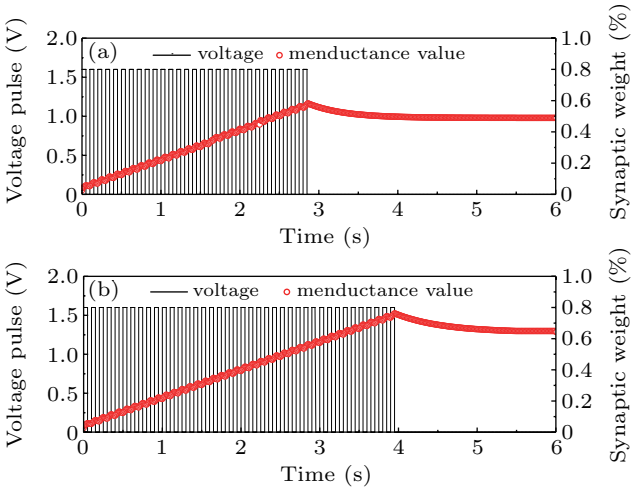


Fig. 6. The effect of different number of pulse stimulation on synaptic weight: (a) the number of pulses is 30, and (b) the number of pulses is 40.

4. Experiential learning

Organisms begin to forget immediately after learning, and the process of forgetting is nonlinear. The rate of forgetting is fast in the beginning, and then it slows down. When the learning is continued after forgetting, it is easier to reach the same memory level. This process is called experiential learning. The following experiments are carried out in order to research the learning behavior of the SBT-memristor-based synapses.

In Fig. 7, the synaptic device is stimulated by 30 pulses at first. The spontaneous forgetting of synaptic weights occurred after learning, which is consistent with the results in Fig. 6(a). In the forgetting process of synaptic devices after the first stimulus, the pulses are applied to SBT-memristor for the second time. The synapse weight can exceed the first value by applying three pulses, and then the forgetting of the synaptic weight occurs again, as shown in Fig. 7.

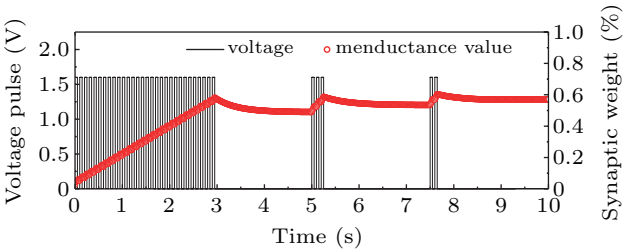


Fig. 7. Experiential learning of the SBT-memristor-based synapses.

In the third time, the synaptic weight can exceed the second value with only two pulses, as shown in Fig. 7. The empirical learning behavior of the SBT-memristor-based synapse device is consistent with the memory rule of Ebbinghaus, which conforms to the memory rule of human brain. As a

result, the SBT-memristor-based synapse can exhibit experiential learning behavior.

5. Non-associative learning

Non-associative learning refers to a change in a behavioral response to a novel stimulus after repeated or continuous exposure to that stimulus. Sensitization and habituation are examples of non-associative learning. Whereas habituation is primarily attributed to activity-dependent synaptic depression, and sensitization is often attributed to the facilitatory actions of neuromodulators.[45,46]

5.1. Habituation

In this part, the influence of pulse frequency on the habituation of the SBT-memristor-based synapse device is studied. The 60 pulses with amplitude of 1.6 V and different frequency (5 Hz, 3 Hz and 2 Hz) are applied on the SBT-memristor, respectively. When the amplitude of the pulse is fixed, the frequency of the pulse is larger, the synaptic weight is smaller (see Fig. 8). The SBT-memristor-based synapse adapts to this harmless stimulation gradually, and its behavioral response weakens. Thus, the SBT-memristor exhibits the process of synaptic habituation. This is because when the frequency of pulse is larger, the time of the memristor with the positive electric field is shorter, resulting in the decrease of the changes of menductance values.

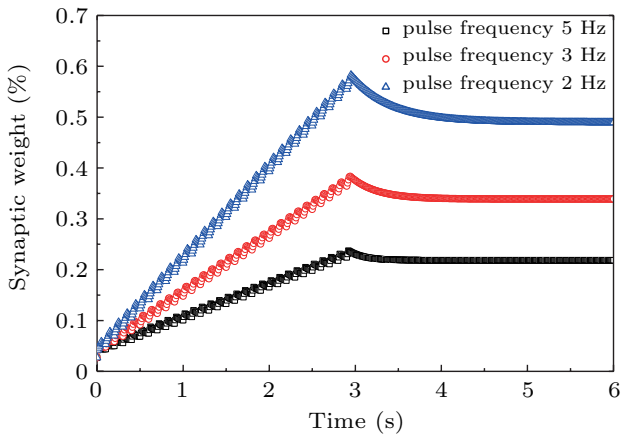


Fig. 8. The influence of different pulse frequency on habituation.

5.2. Sensitization

In this part, the influence of pulse amplitude on the sensitization of the SBT-memristor-based synapse device is studied. Here 30 pulses (2 Hz frequency) with different amplitude (1.3 V, 1.5 V and 1.7 V) are applied on the SBT-memristor, respectively. When the frequency of the pulse is fixed, the amplitude of the pulse is larger, the synaptic weight is larger (see Fig. 9). That is because the external stimulus is stronger, it is easier to cause synaptic excitement and sensitization. Thus, the SBT-memristor exhibits the process of synaptic sensitization. This is because when the amplitude of pulse is larger, the changes of menductance values increases.

Non-associative learning is the basis of many complex learning. By the SBT-memristor-based synapse device, non-associative learning process of human brain are simulated. It shows that the SBT-memristor-based synapse device has the potential to simulate complex learning.

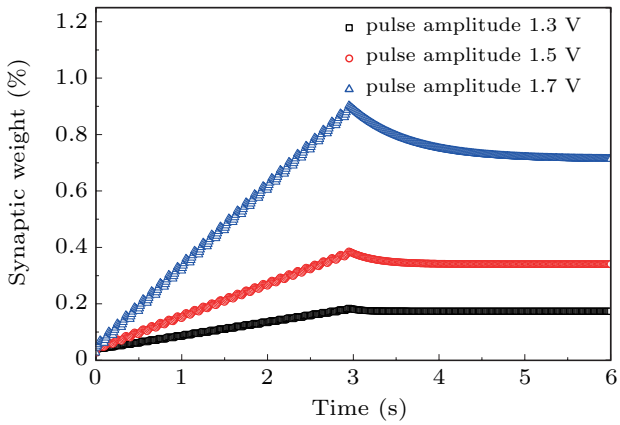


Fig. 9. The influence of different pulse amplitude on habituation.

6. Conclusion

The mathematical model of physical SBT-memristor is established. Based on the SBT-memristor, artificial neural synapse is constructed, which realizes the non-linear transmission characteristics, short-term plasticity and long-term plasticity of the synapse. The experiential learning and non-associative learning behavior in accordance with human cognitive rules are realized by using the SBT-memristor-based synapse. The process of synaptic habituation and sensitization is analyzed. This study provides valuable guidance for the development of artificial neural network.

References

[1] Liu H J, Ma L F, Wang Z D, Liu Y R and Alsaadi F E 2020 *Neurocomputing* **391** 1
[2] Wang J R and Zhuge F 2019 *Adv. Mater. Technol.* **4** 1800544
[3] Li B, Liu Y Q, Wan C J, Liu Z Y, Wang M, Qi D P, Yu J C, Cai P Q, Xiao M, Zeng Y and Chen X D 2018 *Adv. Mater.* **30** 1706395
[4] Ziegler M, Riggert C, Hansen M, Bartsch T and Kohlstedt H 2015 *IEEE Trans. Biomed. Circuits Syst.* **9** 197
[5] Nishitani Y, Kaneko Y and Ueda M 2015 *IEEE Trans. Neural Networks Learn. Sys.* **26** 2999
[6] Li J X, Duan Q X, Zhang T, Yin M H, Sun X H, Cai Y M, Li L D, Yang Y C and Huang R 2017 *RSC Adv.* **7** 43132
[7] Nair M V, Muller L K and Indiveri G 2017 *Nano Futures* **1** 035003
[8] Chen J, Lin C Y, Li Y, Qin C, Lu K, Wang J M, Chen C K, He Y H, Chang T C, Sze S M and Miao X S 2019 *IEEE Electron Device Lett.* **40** 542
[9] Jang B C, Kim S, Yang S Y, Park J, Cha J H, Oh J, Choi J, Im S G, Dravid V P and Choi S Y 2019 *Nano Lett.* **19** 839
[10] Boybat I, Le Gallo M, Nandakumar S R, Moraitis T, Parnell T, Tuma T, Rajendran B, Leblebici Y, Sebastian A and Eleftheriou E 2018 *Nat. Commun.* **9** 2514
[11] Hong Q H, Yan R A, Wang C H and Sun J R 2020 *IEEE Trans. Biomed. Circuits Syst.* **14** 1036

[12] Chua L O 1971 *IEEE Trans. Circ. Theory* **18** 507

[13] Strukov D B, Snider G S, Stewart D R and Williams R S 2008 *Nature* **453** 80

[14] Vincent A F, Larroque J, Locatelli N, Romdhane N B, Bichler O, Gamrat C, Zhao W S, Klein J O, Galdin Retailleau S and Querlioz D 2015 *IEEE Trans. Biomed. Circuits Syst.* **9** 166

[15] He H K, Yang R, Zhou W, Huang H M, Xiong J, Gan L, Zhai T Y and Guo X 2009 *Small* **14** 1800079

[16] Das M, Kumar A, Singh R, Htay M T and Mukherjee S 2018 *Nanotechnology* **29** 055203

[17] Lin Y, Zeng T, Xu H Y, Wang Z Q, Zhao X N, Liu W Z, Ma J Q and Liu Y C 2018 *Adv. Electron. Mater.* **4** 1800373

[18] Feng X W, Li Y D, Wang L, Chen S, Yu Z G, Tan W C, Macadam N, Hu G H, Huang L, Chen L, Gong X, Chi D Z, Hasan T, Thean A V Y, Zhang Y W and Ang K Wee 2020 *Adv. Electron. Mater.* **5** 1900740

[19] Jiang R, Ma P F, Han Z Y and Du X H 2017 *Sci. Rep.* **7** 9354

[20] Chandrasekaran S, Simanjuntak F M, Saminathan R, Panda D and Tseng T Y 2019 *Nanotechnology* **30** 445205

[21] Li S J, Dong B Y, Wang B, Li Y, Sun H J, He Y H, Xu N and Miao X S 2019 *IEEE Trans. Electron Devices* **66** 810

[22] Kim S, Du C, Sheridan P, Ma W, Choi S and Lu W D 2015 *Nano Lett.* **15** 2203

[23] Sokolov A S, Jeon Y R, Kim S, Ku B and Choi C 2019 *NPG Asia Mater.* **11** 5

[24] Kumar M, Ban D K, Kim S M, Kim J and Wong C P 2019 *Adv. Electron. Mater.* **5** 1900467

[25] Chen Z L, Yu Y, Jin L F, Li Y F, Li Q Y, Li T T, Zhang Y T, Dai H T and Yao J Q 2020 *Mater. Des.* **188** 108415

[26] Aghnout S and Karimi G 2019 *Integr VLSI J.* **64** 184

[27] Duan S K, Hu X F, Dong Z K, Wang L D and Mazumder P 2015 *IEEE Trans. Neural Networks Learn. Sys.* **26** 1202

[28] Park S, Chu M, Kim J, Noh J, Jeon M, Hun Lee B, Hwang H, Lee B and Lee B G 2015 *Sci. Rep.* **5** 10123

[29] Hansen M, Zahari F, Ziegler M and Kohlstedt H 2017 *Front. Neurosci.* **11** 91

[30] Liu Q, Wang L D, Yang J, Wang Y and Duan S K 2017 *J. Circuits Syst. Comput.* **26** 1750161

[31] Liu L, Xiong W, Liu Y X, Chen K G, Xu Z, Zhou Y, Han J, Ye C, Chen X, Song Z T and Zhu M 2020 *Adv. Electron. Mater.* **6** 1901012

[32] Prezioso M, Merrikh Bayat F, Hoskins B D, Adam G C, Likharev K K and Strukov D B 2015 *Nature* **521** 61

[33] Covi E, Brivio S, Serb A, Prodromakis T, Fanciulli M and Spiga S 2016 *Front. Neurosci.* **10** 482

[34] Zamarreno Ramos C, Camunas Mesa L, Perez Carrasco J, Masquelier T, Serrano Gotarredona T and Linares Barranco B 2011 *Front. Neurosci.* **5** 26

[35] Serb A, Bill J, Khiat A, Berdan R, Legenstein R and Prodromakis T 2016 *Nat. Commun.* **7** 12611

[36] Hu X F, Feng G, Duan S K and Liu L 2017 *IEEE Trans. Neural Networks Learn. Sys.* **28** 1889

[37] Dou G, Yu Y, Guo M, Zhang Y M, Sun Z and Li Y X 2017 *Chin. Phys. Lett.* **34** 126

[38] Zhang Y M, Dou G, Sun Z, Guo M and Li Y X 2017 *Int. J. Bifurcation Chaos* **27** 1750148

[39] Chang T, Jo S H, Kim K H, Sheridan P, Gaba S and Lu W 2011 *Appl. Phys. A* **102** 857

[40] Meng F Y, Duan S K, Wang L D, Hu X F and Dong Z K 2015 *Acta Phys. Sin.* **64** 148501 (in Chinese)

[41] Li Y, Zhong Y P, Zhang J J, Xu L, Wang Q, Sun H J, Tong H, Cheng X M and Miao X S 2014 *Sci. Rep.* **4** 4906

[42] Liu G, Wang C, Zhang W B, Pan L, Zhang C C, Yang X, Fan F, Chen Y and Li R W 2016 *Adv. Electron. Mater.* **2** 1500298

[43] Xiao Z G and Huang J S 2016 *Adv. Electron. Mater.* **2** 1600100

[44] Mori M, Abegg M H, Gahwiler B H and Gerber U 2004 *Nature* **431** 453

[45] Byrne J H and Hawkins R D 2015 *CSH Perspect. Biol.* 7 a021675

[46] Van De Burgt Y, Lubberman E and Fuller E J 2017 *Nat. Mater.* **16** 414